On Determining the Structure of a Medium Using a Multi-Fold Seismic Observation System

*G. F. Zherniak**

Translated by Chuck Sword

In this work is examined the problem of reconstructing the structure of a medium, using the full wave field obtained by an observation system of multi-fold coverage. Algorithms are described which allow one to determine the structure of a medium, when several assumptions are made about the form of the wavefield in it. Variants of lineal (2-D) and areal (3-D) observation systems are examined. Results are presented of testing the algorithms on data from numerical models.

In connection with the increasing difficulty of the problems being solved by exploration seismology, there has arisen the need for processing methods which more fully take into account the dynamics of the seismic wavefield, and which are suitable for media that have a substantially three-dimensional structure. At the present time, wide distribution has been given to procedures for obtaining depth sections based on methods of wave migration. These procedures are usually applied to multi-fold data that has already been CDP stacked. Because of this, the use of migration when steeply-dipping boundaries are present proves to be ineffective. This is connected with distortions in the wavefield caused by CDP summation, as well as with the discrepancy between the CDP-stacked time section and the zero-offset experiment assumed by most migration algorithms. Particular difficulties arise in the use of these methods in substantially three-dimensional media, when the depth sections obtained along various traverse lines agree poorly with each other.

In the present work is examined the problem of obtaining an image of the medium directly from the data of various forms of multi-fold seismic observation. The redundant information provided by similar systems is used to increase the stability of the image and to filter out wave-noise.

Dr. Zherniak is a researcher at the Computing Center of the Siberian Branch of the USSR Academy of Sciences, in the city of Novosibirsk. This article was sent to us by Dr. Zherniak in the form of a preprint.

Let us look at the equation

$$\Delta U - \frac{1}{v^2(R)} U_{tt} = -\delta(R-R_0) f(t); \tag{1}$$

$$R = (x, y, z), \quad R_0 = (x_0, y_0, z_0),$$

which describes the propagation of waves excited by a source at point R_0, in a medium characterized by a velocity $v(R)$. Having obtained some velocity $v_0 = const$, we present equation (1) in the form

$$\Delta U - \frac{1}{v_0^2} U_{tt} = -\delta(R-R_0) f(t) - \tilde{c}(R) \frac{1}{v_0^2} U_{tt}; \tag{2}$$

$$\tilde{c}(R) = 1 - \frac{v_0^2}{v^2}.$$

Let the signal emitted by the source, $f(t) = 0$ for $t < 0$, and let the velocity function $\tilde{c}(R) = 0$ outside some closed area D.

Having performed a time-domain Fourier transform, we give the resulting Helmholtz equation in integral form [4]:

$$U(R, R_0, k) = \Phi(kv_0) \frac{e^{-ik|R-R_0|}}{4\pi|R-R_0|} - \tag{3}$$

$$- \frac{k^2}{4\pi} \int_D \tilde{c}(R_1) U(R_1, R_0, k) \frac{e^{-ik|R-R_1|}}{4\pi|R-R_1|} dR_1,$$

where $k = \omega / v_0$ is the wave number, and $\Phi(\omega)$ is the spectrum of the signal $f(t)$. The radiation conditions are assumed to be fulfilled.

Let there be, at surface $z = 0$, a recorded field $U(R, R_0, t)$, excited by sources on the surface $z_0 = const$. We will assume that the signal $f(t)$ is known and that the inhomogeneous area D lies lower than the surfaces $z = 0$ and z_0. Then the frequency spectrum of the observed field is determined according to (3), which will be looked upon as an integral equation concerning the unknown velocity function $\tilde{c}(R)$.

The first term on the right side of equation (3) corresponds to the observed direct wavefield from the sources, and under known conditions of shooting and recording it can be removed from the recorded data. The field in the medium, $U(R_1, R_0, k)$, which enters into the expression under the integral, is unknown and depends on the structure of the medium, $\tilde{c}(R_1)$, which in its turn must be determined. In connection with this it is necessary to specify an assumption about the field in the medium, an assumption which naturally narrows the set of allowed models $\tilde{c}(R)$.

We will assume that in several sub-volumes $D_1 \subset D$, this expression is appropriate:

$$U(R_1, R_0, k) = \Phi(kv_0)\frac{e^{-ik|R_1-R_0|}}{4\pi|R_1-R_0|} + U_1(R_1, R_0, k), \tag{4}$$

that is, the field in the medium has a composition similar to the field due to a point source in a homogeneous volume. This condition, under which the secondary field U_1 can be neglected in the case of weak scattering, is called the Born-Rayleigh approximation, and the possibility of its use for the solution of an equation in the form of (3) has been investigated by a series of authors. In works [8] and [9] it was formally used for the construction of algorithms to determine the velocity structure of a medium, based on solving the integral equations. However, as was shown in [5], when the conditions for applying the Born approximation are strongly adhered to, there arise substantial limitations not only on the deviation of the velocity function from its mean value, but on the size of the inhomogeneous area D as well. Because of this, only a few functionals of $\tilde{c}(R)$ yield a stable determination.

Here we will not require that the secondary field U_1 be small in the medium, and its influence will be looked upon as an effect of regular noise. Fundamental to posing the problem in this way are both the redundant information in the data, the presence of which allows us to filter out the noise field, and our experience with using the CDP method, which accomplishes a similar filtration. However, in the problem posed thus, we will determine not the velocity function $\tilde{c}(R)$, but some image of it, $c(R)$, an image which reflects the peculiarities in the structure of the medium. This is connected with the fact that the secondary field U_1 can have elements that are similar to the direct field, and the effect of these elements is not suppressed by filtration [5].

Taking into account all of these assumptions, we write the observed field in the form:

$$U(r, r_0, k) = -\frac{k^2\Phi(kv_0)}{(4\pi)^2}\int_{D_1} c(R_1)\frac{e^{-ik|R_1-R_0|}}{|R_1-R_0|}\,\frac{e^{-ik|r-R_1|}}{|r-R_1|}\,dR_1 + \tilde{U}(r, r_0, k),$$

$$r = (x, y), \quad r_0 = (x_0, y_0), \tag{5}$$

$$|R_1-R_0| = \left[(x_1-x_0)^2 + (y_1-y_0)^2 + (z_1-z_0)^2\right]^{1/2},$$

and we will look upon the second term in the integral equation (5) as regular noise, produced both by secondary interactions and by radiation from the area outside of D_1.

We will examine two different variants of a system of observation.

Observational Variant I

The shots and receivers are laid out over the whole area, and they are laid out independently. That is, a five-dimensional wavefield is recorded, the temporal spectrum of which will be described by equation (5). When we don't consider the noise field, performing a Fourier transform on (5) over the variables r and r_0 gives us

$$U(\kappa, \kappa_0, k) = F_{r, r_0}\left[U(r, r_0, k)\right] =$$

$$\frac{k^2\Phi(k\upsilon_0)}{4}\int_{-\infty}^{\infty} c(\kappa+\kappa_0, z_1)\frac{e^{\mp i[(z_1-z_0)\sqrt{k^2-\kappa_0^2}+z_1\sqrt{k^2-\kappa^2}]}}{\sqrt{k^2-\kappa_0^2}\cdot\sqrt{k^2-\kappa^2}}dz_1, \qquad (6)$$

$$\kappa = (\kappa_x, \kappa_y), \quad \kappa_0 = (\kappa_{x0}, \kappa_{y0}).$$

Here we used the formula for the spectrum of the fundamental solution [3]

$$F_r\left[\frac{e^{-ik|R|}}{|R|}\right] = \mp 2\pi i\frac{e^{\mp i|z|\sqrt{k^2-\kappa^2}}}{\sqrt{k^2-\kappa^2}} \qquad (7)$$

and we took into account the condition that $c(\kappa+\kappa_0, z_1) = 0$ for $z_1 < 0$, $z_1 < z_0$. The upper sign in (6) and (7) corresponds to the case $k > 0$.

We introduce the focusing function for plane z:

$$\Psi(\kappa, \kappa_0, k, z) = \frac{2\Pi(\kappa/k)\Pi(\kappa_0/k)}{\pi\Phi(k\upsilon_0)}\frac{\sqrt{k^2-\kappa_0^2}+\sqrt{k^2-\kappa^2}}{|k|}e^{\pm i[(z-z_0)\sqrt{k^2-\kappa_0^2}+z\sqrt{k^2-\kappa^2}]}. \qquad (8)$$

The function $\Pi(x)$ is defined as:

$\Pi(x) = 1$ for $|x| \le 1$, $\Pi(x) = 0$ for $|x| > 1$.

Let us look at the integral transformation of the spectrum of the observed field

$$W(\kappa, \kappa_0, z) = \int_{-\infty}^{\infty} U(\kappa, \kappa_0, k)\Psi(\kappa, \kappa_0, k, z)\,dk. \qquad (9)$$

The presence of the factor $\Pi(\kappa/k)$ in the kernel (8) of the transformation (9) indicates that only the homogeneous planar waves of the spatial spectrum are used. We will use the representation in (7) for $U(\kappa, \kappa_0, k)$, and introducing the symbols

$$k_r = \kappa + \kappa_0, \quad \gamma = \kappa - \kappa_0,$$

$$\alpha = \left[k^2 - (k_r+\gamma)^2/4\right]^{1/2}, \quad \beta = \left[k^2 - (k_r-\gamma)^2/4\right]^{1/2},$$

we will write (9) in the form

$$W(k_r, z, \gamma) = \frac{1}{2\pi}\int_{-\infty}^{\infty}\int c(k_r, z_1)\Pi\left(\frac{k_r+\gamma}{2k}\right)\Pi\left(\frac{k_r-\gamma}{2k}\right)\times \tag{10}$$

$$\times\frac{|k|(\alpha+\beta)}{\alpha\cdot\beta}e^{\mp i(z_1-z)(\alpha+\beta)}\,dz_1\,dk.$$

In order to investigate the integral transformation of the field we will apply to relation (10) a Fourier transform over z, which gives us

$$W(\nu, \gamma) = \int_{-\infty}^{\infty} c(\nu)\Pi\left(\frac{k_r+\gamma}{2k}\right)\Pi\left(\frac{k_r-\gamma}{2k}\right)\frac{|k|(\alpha+\beta)}{\alpha\beta}\delta(k_z \mp(\alpha+\beta))\,dk, \tag{11}$$

where $\nu = (k_r, k_z) = (k_x, k_y, k_z)$.

In order to integrate over k we will transform the δ-function from (11) using the formula [4]

$$\delta(\varphi(k)) = \sum_n \frac{\delta(k-k_n)}{|\varphi'(k_n)|},$$

where k_n are the roots of the equation

$$\varphi(k) = k_z \mp\left[\left(k^2-(k_r+\gamma)^2/4\right)^{1/2} + \left(k^2-(k_r-\gamma)^2/4\right)^{1/2}\right]$$

with regard to k.

Having taken into account the correspondence between the signs ($\mp$) in the given δ-function and the sign of k, we find

$$\delta(k_z \mp(\alpha+\beta)) = \Pi\left(\frac{k_r\gamma}{k_z^2}\right)\left|\frac{\alpha\beta}{k(\alpha+\beta)}\right|_{k=k_{1,2}}\delta(k-k_{1,2}), \tag{12}$$

$$\text{where}\quad k_{1,2} = \mp\left(\frac{(k_r\gamma)^2 + k_z^2(k_r^2+\gamma^2) + k_z^4}{4k_z^2}\right)^{1/2}$$

After we integrate over k we obtain

$$W(\nu, \gamma) = c(\nu)\Pi\left(\frac{k_r+\gamma}{2k_{1,2}}\right)\Pi\left(\frac{k_r-\gamma}{2k_{1,2}}\right)\Pi\left(\frac{k_r\gamma}{k_z^2}\right). \tag{13}$$

After we express the product of the first two Π-functions in (13) in the form of an equivalent system of inequalities

$$\Pi\left(\frac{k_r+\gamma}{2k_{1,2}}\right)\Pi\left(\frac{k_r-\gamma}{2k_{1,2}}\right) \Rightarrow \begin{cases} |k_r+\gamma| \le \sqrt{k_r^2+k_z^2+\gamma^2+(k_r\gamma)^2/k_z^2} \\ |k_r-\gamma| \le \sqrt{k_r^2+k_z^2+\gamma^2+(k_z\gamma)^2/k_z^2} \end{cases} \Rightarrow$$

$$=> \frac{k_z^2}{|k_r\gamma|} + \frac{|k_r\gamma|}{k_z^2} \geq 2 \quad \text{for all} \quad \frac{k_z^2}{|k_r\gamma|}, \tag{14}$$

we find that

$$\Pi\left(\frac{k_r+\gamma}{2k_{1,2}}\right)\Pi\left(\frac{k_r-\gamma}{2k_{1,2}}\right) = 1,$$

and consequently

$$W(\nu, \gamma) = c(\nu)\Pi\left(\frac{k_r\gamma}{k_z^2}\right). \tag{15}$$

In this manner, the function $W(\nu, \gamma)$, determined by the transformation in (9), coincides with the spectrum of the image of the medium $c(\nu)$, for all γ that satisfy the inequality $|k_r\gamma| \leq k_z^2$. Thus γ represents a free parameter, since the spectrum of our sought-for function $c(\nu)$ doesn't depend on it. At the same time the noise field from (5), which by assumption is not described by the integral representation that we used, becomes, as a result of the transformation, dependent on γ. Therefore integrating $W(\nu, \gamma)$ over γ (which corresponds to low-frequency filtering) must lead to a stacking of the signals described by our model, relative to the noise field. So, after we perform the integration with a weighting function $k_r / 2k_z^2$, to compensate for the inhomogeneity of the stacking, we obtain

$$W_1(\nu) = \frac{1}{2k_z^2}\int_{-\infty}^{\infty} W(\nu, \gamma)\cdot(k_r \cdot d\gamma) = c(\nu). \tag{16}$$

The inverse Fourier transform of the function $W_1(\nu)$ restores in area D_1 an image of the medium $c(R)$, complicated by the remaining regular noise. To calculate the intensity and area of dissemination of the noise in the general case is difficult. However, an extremely simple scheme is used in the CDP method for stacking redundant information, and our experience in applying this scheme confirms the possibility of suppressing wave noise, in particular, multiple noise.

Because the solution was obtained using the given assumptions about the wavefield in the medium, the direct use of this algorithm is well-grounded for those parts of the medium where the field due to the sources is similar to the sources' direct field in a homogeneous space. An example of such a model is a layered-inhomogeneous medium with curvilinear (optionally smooth) boundaries and sufficiently small velocity inhomogeneities within the layers. In this case it is possible to obtain an image of the medium right up to the "strong" upper boundary S_1, and to obtain the position of the boundary itself. Afterwards, with the help of a full recalculation of the field over the receivers and sources, it is possible to

approximately transfer the entire system of observations to the boundary S_1, which makes it possible to use the algorithm for determining the structure of the next layer, and so on. We should note that the operator for the recalculation of the field of homogeneous planar waves, which is used in this algorithm, enters into the focusing function (8), guaranteeing the stable continuation of the field in the medium, within the framework of the algorithm. The values of the mean velocities in the layers might be obtained either from a well log, or from some selection method analogous to the "velocity spectrum" algorithm in the CDP method.

In the resulting algorithm it is possible to take into account the condition when the surface of observation is the boundary of the section. For instance, in the case when the surface of observation $z = 0$ is a free surface, on which $U(R, R_0, k) = 0$, and the normal derivative of the field, $U_z(R, R_0, k)|_{z=0}$ is measured. For a sufficiently small source depth z_0, the radiation function takes on the form

$$G_{z0}(R, R_0, k) \approx 2z_0 \frac{\partial}{\partial z_0}\left[\frac{e^{-ik|R-R_0|}}{4\pi|R-R_0|}\right], \tag{17}$$

and equation (5) for the observed normal derivative of the field is

$$U_z(r, r_0, k) \approx -\frac{k^2\Phi(kv_0)}{2z_0}\int_{D_1} c(R_1)G_{z0}(r_0, R_1, k)G_z(r, R, k)dR_1 + \tilde{U}(r, r_0, k). \tag{18}$$

In order to obtain a solution of the same form it is necessary to introduce the previously-described transformations, introducing into the focusing function the supplementary multiplier

$$1/\left(2z_0\sqrt{k^2-\kappa_0^2}\cdot\sqrt{k^2-\kappa^2}\right).$$

In the case of the planar (2-D) problem the spectrum of the fundamental solution of the Helmholtz equation has the form

$$F_x\left[-\frac{i}{4}H_0^{(2)}(k\sqrt{z^2+x^2})\right] = \mp\frac{i\,e^{\mp i|z|\sqrt{k^2-k_x^2}}}{2\sqrt{k^2-k_x^2}}, \tag{19}$$

where k_x is the spatial frequency corresponding to the vector κ from the three-dimensional case. That is, (19) has the same form as (6) does. Because of this, the method can be transferred to the planar case, which simplifies the study of several general characteristics of the algorithm.

Observational Variant II

The implementation of the full areal (3-D) system of observation described above gives rise to a series of difficulties of a quantitative nature. In connection with this, there is a practical significance to the problem of modifying the algorithm for areal observation systems which provide information of a lower dimensionality.

Let the sources and receivers of the field be located on the plane $z = z_0 = 0$, and let there be implemented a system of parallel profiles with multi-fold coverage. That is, for each profile let the value of the field be recorded only on the straight line $y = y_0$, which is the line along which the source travels. Such an observation system, while still redundant, gives data of one less dimension. The observed four-dimensional field, taking into account the assumptions introduced previously, is described by relationship (5), but with $z = z_0 = 0$, $y = y_0$, to wit:

$$U(x, x_0, y, k) = -\frac{k^2\Phi(kv_0)}{(4\pi)^2}\int_{D_1} c(R_1)\frac{e^{-ik\sqrt{(x_1-x_0)^2+(y_1-y)^2+z_1^2}}}{\sqrt{(x_1-x_0)^2+(y_1-y)^2+z_1^2}}\times \tag{20}$$

$$\times\frac{e^{-ik\sqrt{(x-x_1)^2+(y-y_1)^2+z_1^2}}}{\sqrt{(x-x_1)^2+(y-y_1)^2+z_1^2}}dR_1 + \tilde{U}(x, x_0, y, k)\,.$$

In order to obtain a solution, let us carry out the sequence of transformations analogous to (6) - (16).

Let us introduce the Fourier transform of equation (20) over the coordinates x and x_0 of the receivers and shots:

$$U(\kappa, \kappa_0, y, k) = F_{x,x_0}[U(x, x_0, y, k)] =$$

$$= \frac{k^2\Phi(kv_0)}{16}\int_{D_1}\int c(\kappa+\kappa_0, y_1, z_1)H_0^{(2)}\left[\sqrt{z_1^2+(y_1-y)^2}\sqrt{k^2-\kappa^2}\right]\times \tag{21}$$

$$\times H_0^{(2)}\left[\sqrt{z_1^2+(y-y_1)^2}\sqrt{k^2-\kappa_0^2}\right]dy_1\,dz_1\,.$$

Here we used the equation from [7]

$$F_x\left[\frac{e^{-ik\sqrt{a^2+x^2}}}{\sqrt{a^2+x^2}}\right] = -\pi i\,H_0^{(2)}\left[a\sqrt{k^2-\kappa^2}\right], \quad a>0, \quad \kappa=\kappa_x\,.$$

The integral over y_1 in (21) is a convolution integral, and therefore, after we perform the Fourier transform over the profile coordinate y, we obtain

$$U(\kappa, \kappa_0, k_y, k) = \frac{k^2\Phi(kv_0)}{16}\int_{-\infty}^{\infty} c(\kappa+\kappa_0, k_y, z_1)G(\kappa, \kappa_0, k_y, z_1, k)dz_1\,, \tag{22}$$

where $G(\kappa, \kappa_0, k_y, z_1, k) = F_y\left[H_0^{(2)}\left(\alpha\sqrt{y^2+z_1^2}\right)H_0^{(2)}\left(\beta\sqrt{y^2+z_1^2}\right)\right]$,

$$\alpha = \sqrt{k^2 - \kappa^2}, \quad \beta = \sqrt{k^2 - \kappa_0^2}.$$

Let us determine the spectrum of the product of the Hankel functions in (22), in the area $\alpha^2 > 0$, $\beta^2 > 0$, $(\alpha+\beta) \geq k_y^2$. We will use the formulas from [6, 7]

$$H_0^{(2)}(x)H_0^{(2)}(y) = \frac{2i}{\pi}\int_{-\infty}^{\infty} H_0^{(2)}\left(\sqrt{x^2 + y^2 + 2xy\,\mathrm{ch}(2t)}\right)dt,$$

$$F_y\left[H_0^{(2)}\left(b\sqrt{y^2 + a^2}\right)\right] = 2\frac{e^{-i|a|\sqrt{b^2-k_y^2}}}{\sqrt{b^2-k_y^2}}$$

and we represent this spectrum in the form

$$G(\kappa, \kappa_0, k_y, z_1, k) = \frac{2i}{\pi}\int_{-\infty}^{\infty} \frac{e^{-i|z_1|\sqrt{\alpha^2 + \beta^2 + 2\alpha\beta\mathrm{ch}(t) - k_y^2}}}{\sqrt{\alpha^2 + \beta^2 + 2\alpha\beta\mathrm{ch}(t) - k_y^2}}\,dt. \tag{23}$$

This last integral can be approximated with the help of the method of stationary phases, assuming here that $kz_1 \gg 1$, [3], that is, assuming that the distance to the area D_1 is very much greater than the wavelength $\lambda = 2\pi/k$. The estimate for the function G, obtained with these conditions, has the form

$$G(\kappa, \kappa_0, k_y, z_1, k) \approx \left(\frac{8}{\pi z_1}\right)^{1/2} \frac{e^{-i(|z_1|\sqrt{(\alpha+\beta)^2-k_y^2} - \pi/4)}}{\left(\alpha\beta\sqrt{(\alpha+\beta)^2-k_y^2}\right)^{1/2}}. \tag{24}$$

Expression (24) was obtained for $k > 0$, but from the properties of the Fourier transform it follows that

$$G(\kappa, \kappa_0, k_y, z_1, k < 0) = G^*(-\kappa, -\kappa_0, -k_y, z_1, k > 0),$$

so that in any case it reduces to a change of the sign in front of the index of the exponent in (24).

Having obtained an expression for the spectrum G in (22), and having taken into account the condition that $c(R) = 0$ for $z < 0$, we obtain the relation

$$U(\kappa, \kappa_0, k_y, k) \approx \frac{k^2\Phi(k\upsilon_0)}{4\sqrt{2\pi}}\int_{-\infty}^{\infty} \frac{c(\kappa+\kappa_0, k_y, z_1)}{\sqrt{z_1}} \frac{e^{\mp i\left(z_1\sqrt{(\alpha+\beta)^2-k_y^2} - \pi/4\right)}}{\left(\alpha\beta\sqrt{(\alpha+\beta)^2-k_y^2}\right)^{1/2}}\,dz_1, \tag{25}$$

which approximately expresses the space-time spectrum of the observed field.

Let us define the focusing function as

$$\Psi(\kappa, \kappa_0, k_y, k, z) = \tag{26}$$

$$\frac{4e^{\mp i\pi/4}}{\sqrt{2\pi}\,|k|\,\Phi(k v_0)}\left[\Pi\left(\frac{\kappa}{k}\right)\Pi\left(\frac{\kappa_0}{k}\right)\Pi\left(\frac{k_y}{\alpha+\beta}\right)\frac{(\alpha+\beta)^2 e^{\pm i z\sqrt{(\alpha+\beta)^2-k_y^2}}}{\left[\alpha\beta\sqrt{(\alpha+\beta)^2-k_y^2}\right]^{1/2}}\right],$$

in which the product of the Π functions expresses the limits on α, β, and k_y that were imposed earlier.

When we put into the integral transform (9) the expression just obtained for the wave-field and the function Ψ, and make the change of variables $k_x = \kappa + \kappa_0$, $\gamma = \kappa - \kappa_0$, we find that

$$W(k_x, k_y, z, \gamma) = \frac{1}{2\pi}\int_{-\infty}^{\infty}\int c_1(k_x, k_y, z_1)\Pi\left(\frac{k_x+\gamma}{2k}\right)\Pi\left(\frac{k_x-\gamma}{2k}\right)\Pi\left(\frac{k_y}{\alpha+\beta}\right)\times \tag{27}$$

$$\times\frac{|k|(\alpha+\beta)^2 e^{\mp i(z_1-z)\sqrt{(\alpha+\beta)^2-k_y^2}}}{\alpha\beta\sqrt{(\alpha+\beta)^2-k_y^2}}\,dz_1\,dk\,,$$

where $c_1(k_x, k_y, z_1) = c(k_x, k_y, z_1)/\sqrt{z_1}$.

Let us apply a Fourier transform over z to relation (27)

$$W(\nu, \gamma) = F_z\left[W(k_x, k_y, z, \gamma)\right] = \tag{28}$$

$$= \int_{-\infty}^{\infty} c_1(\nu)\Pi\left(\frac{k_x+\gamma}{2k}\right)\Pi\left(\frac{k_x-\gamma}{2k}\right)\Pi\left(\frac{k_y}{\alpha+\beta}\right)\frac{|k|(\alpha+\beta)^2\delta\left[k_z \mp\sqrt{(\alpha+\beta)^2-k_y^2}\right]}{\alpha\beta\sqrt{(\alpha+\beta)^2-k_y^2}}$$

$$\nu = (k_x, k_y, k_z)\,.$$

As a result of transforming the δ-function in (28) we obtain

$$\delta\left[k_z \mp\sqrt{(\alpha+\beta)^2-k_y^2}\right] = \delta(k-k_{1,2})\Pi\left(\frac{k_x\gamma}{\mu^2}\right)\left|\frac{\alpha\beta\sqrt{(\alpha+\beta)^2-k_y^2}}{k(\alpha+\beta)^2}\right|_{k=k_{1,2}}, \tag{29}$$

$$\mu^2 = k_y^2 + k_z^2\,,\quad k_{1,2} = \pm\left[\frac{k_x^2\gamma^2 + \mu^2(k_x^2+\gamma^2) + \mu^4}{4\mu^2}\right]^{1/2}.$$

Having obtained, with the help of (29), an integration over k, we find

$$W(\nu, \gamma) = c_1(\nu)\Pi\left(\frac{k_x+\gamma}{2k_{1,2}}\right)\Pi\left(\frac{k_x-\gamma}{2k_{1,2}}\right)\Pi\left(\frac{k_y}{\alpha+\beta}\right)\Pi\left(\frac{k_x\gamma}{\mu^2}\right). \tag{30}$$

When we represent the Π functions from (30) as a system of inequalities we obtain

$$\Pi\left[\frac{k_x+\gamma}{2k_{1,2}}\right]\Pi\left[\frac{k_x-\gamma}{2k_{1,2}}\right]=1,$$

$$\Pi\left[\frac{k_x\gamma}{\mu^2}\right]\Pi\left[\frac{k_y}{\alpha+\beta}\right]_{k=k_{1,2}}= \tag{31}$$

$$=\Pi\left[\frac{k_x\gamma}{\mu^2}\right]\Pi\left[\frac{2\mu k_y}{|k_x\gamma-\mu^2|+|k_x\gamma+\mu^2|}\right]=\Pi\left[\frac{k_x\gamma}{\mu^2}\right].$$

Consequently,

$$W(\nu,\gamma)=c_1(\nu)\Pi\left[\frac{k_x\gamma}{\mu^2}\right]. \tag{32}$$

This is the relationship whose form coincides with (15). Integrating (32) over the free parameter γ, we obtain the spectral function of the image

$$W_1(\nu)=\frac{|k_x|}{2\mu^2}\int_{-\infty}^{\infty}W(\nu,\gamma)d\gamma=c_1(\nu), \tag{33}$$

and the inverse Fourier transform from which we reconstruct the image of the media is

$$F_\nu^{-}\left[W_1(\nu)\right]=c(R)/\sqrt{z}. \tag{34}$$

Let us particularly examine the case when the spectrum of the signal $\Phi(\omega)$ is determined only in the finite band of frequencies $|\omega|\le\Omega$. Let us assume that $\Phi(\omega)=0$ for $|\omega|>\Omega$, and let us change the deconvolution multiplier $1/\Phi(k v_0)$ in (26) to $\Pi(k/K)\Phi(k v_0)$, where $K=\Omega/v_0$. Upon performing the integration over k, we find

$$W(\nu,\gamma,K)=c_1(\nu)\Pi\left[\frac{k_x\gamma}{\mu^2}\right]\Pi\left[\frac{\sqrt{\mu^2+k_x^2+\gamma^2+k_x^2\gamma^2/\mu^2}}{2K}\right]. \tag{35}$$

Let us represent relation (35) in the form of a system of inequalities:

$$W(\nu,\gamma,K)=\begin{cases} c_1(\nu) & \text{for } |\gamma|\le\mu^2/|k_x|,\ |\gamma|\le\mu\sqrt{4K^2/|\nu|^2-1} \\ 0 & \text{for } |\nu|>2K \end{cases} \tag{36}$$

In the coordinates $k_x=|\nu|\cos(\varphi,\mu)=|\nu||\sin\varphi|$ the system of inequalities (36) decomposes into different inequalities for different areas

$$W(\nu, \gamma, K) = \begin{cases} c_1(\nu) & \text{for } |\gamma| \le |\sin\varphi|\sqrt{4K^2-\nu^2},\ 2K|\cos\varphi| \le |\nu| \le 2K \\ c_1(\nu) & \text{for } |\gamma| \le |\nu|\sin^2\varphi/|\cos\varphi|,\ |\nu| < 2K|\cos\varphi| \\ 0 & \text{for } |\nu| > 2K \end{cases} \tag{37}$$

After integrating form (33) over γ we obtain

$$W(\nu, K) = \begin{cases} c_1(\nu) & \text{for } |\nu| < 2K|\cos\varphi| \\ c_1(\nu)|\cot\varphi|\sqrt{4K^2/\nu^2 - 1} & \text{for } 2K|\cos\varphi| \le |\nu| \le 2K \\ 0 & \text{for } |\nu| > 2K \end{cases} \tag{38}$$

Relation (38) shows that the non-zero values of $W_1(\nu, K)$ are concentrated in a sphere of radius $2K$, from which it is possible to make an estimate of the resolving capability of the image, and which allows us to construct an inverse filter for the optimal reconstruction of $c_1(R, K)$. Besides this, the solution for a finite range of frequencies can be the formal basis for allowing the transform that we are examining. We should note that the analogous estimate of the effect of band-limiting the spectrum of the signal can be done for the case of a full system of observations as well.

In the particular case when the velocity function does not depend on the variable y, that is, when the structure of the medium doesn't change perpendicular to the profile, in order to solve to solve the imaging problem it is sufficient to have the data recorded along one profile. Equation (20) is written in this case in the form

$$U_1(x, x_0, k) = U(x, x_0, y, k)_{y=0} = -\frac{k^2\Phi(kv_0)}{(4\pi)^2}\int_{D_1} c_1(x_1, z_1)\frac{e^{-ik\sqrt{(x_1-x_0)^2+y_1^2+z_1^2)}}}{\sqrt{(x_1-x_0)^2+y_1^2+z_1^2)}}\times$$

$$\times\frac{e^{-ik\sqrt{(x-x_1)^2+y_1^2+z_1^2)}}}{\sqrt{(x-x_1)^2+y_1^2+z_1^2)}}dR_1 + \tilde{U}(x, x_0, y, k)\,. \tag{39}$$

and its spatial spectrum

$$U_1(\kappa, \kappa_0, k) = \frac{k^2\Phi(kv_0)}{16}\int_{-\infty}^{\infty} c(\kappa+\kappa_0, z_1)\times \tag{40}$$

$$\times\int_{-\infty}^{\infty} H_0^{(2)}\left(\alpha\sqrt{z_1^2+y_1^2}\right)H_0^{(2)}\left(\beta\sqrt{z_1^2+y_1^2}\right)dy_1\,dz_1\,.$$

The inner integral in (40) is equal to the previously-calculated Fourier transform of the product of the Hankel functions with $k_y = 0$. Consequently, the results we have obtained can be applied to this particular case, if in the equations elucidated above we assume $k_y = 0$, $|\mu| = |k_z|$.

The described approach to the problem of determining the structure of the medium, while remaining limited by the framework of the wave equation, just as the CDP and wave migration methods are, can in principle be applied to the processing of data from the observation of real seismic wavefields. Thus a relative widening of the class of models of media, and an allowance of sorts for the dynamics of wave processes, can turn out to be substantial in the case of a complexly-structured medium.

Numerical Experiments

Without touching on the particularities of applying the algorithms to data from finite and discrete observation systems, let us look at the results of applying them to material from the numerical modeling of wave processes. On the basis of the schemes described, experimental programs were developed for the two-dimensional and three-dimensional variants of the problem. In connection with the processing of synthetic fields, the two-dimensional case was researched in more detail, since it is simpler in its numerical implementation, but it reflects the possibilities of the three-dimensional variant of the algorithm.

Model 1. Two homogeneous flat layers over a half-space, with velocities 2, 2.5, and 3 km/sec respectively. The observation system: 60 receivers 50 m apart, lying on the free surface of the uppermost layer, and 60 sources at a depth of 100 m below the receivers. The length of the layers: 800 m.

The calculation of the wavefield was carried out with the help of a program that numerically solved the wave-equation forward dynamic problem by the method of the incomplete division of changes. Because of the great depth of the buried sources, there appeared, reflected from the free surface, a ghost wave, with an intensity close to that of the direct field in the medium [11].

The temporal wave field computed at the observation points was decomposed into 100 harmonic components in the range 6 to 30 Hz. The images were formed on an orthogonal grid made up of 64×64 elements with steps $\Delta x = \Delta z = 50$ m, for two variants of the velocity v_0. In the first case the velocity was chosen to be equal to the velocity in the upper layer -- 2 km/sec. In this case, by the conditions of the algorithm, the waves reflected from the lower boundary of the second layer turned into regular noise. In the image (fig. 1), only the upper boundary of the second layer was reconstructed clearly, and the images of the lower layer

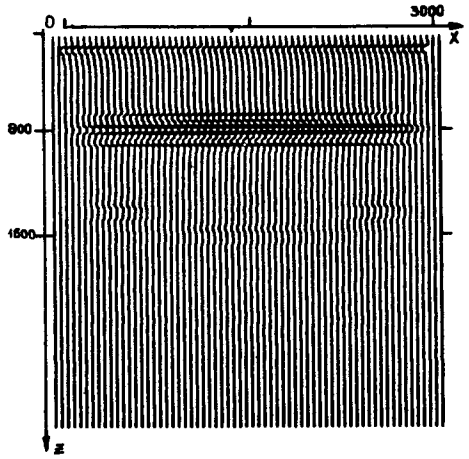

FIG. 1. Image of the medium (in model 1), reconstructed with v_0 = 2 km/sec.

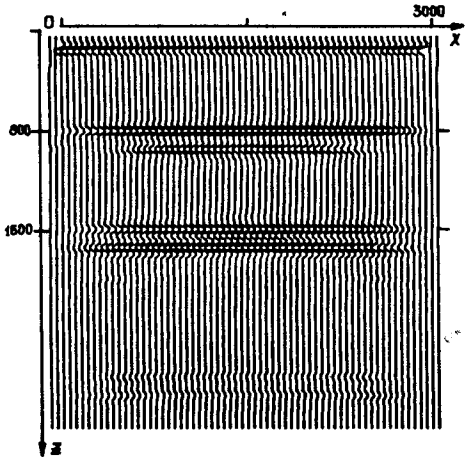

FIG. 2. Image of the medium (in model 1) with $v_0 = v_{avg}(z)$.

and the field of the multiple waves cancelled out. In the second case, by analogy with wave migration, a model with an average velocity depending on depth, $v = v_{avg}(z)$, was used. Both boundaries were reconstructed in the image, and under them can be observed noise images, corresponding to the reflected ghost wave (fig. 2). We note that in the first case, the suppression of these reflections was carried out by means of the method of correlated filtering.

For a comparison to these results, the seismograms were CDP sorted, and they were processed by the method of "CDP stacking, wave migration". The spatial-frequency variant of migration was used, with $v_{avg}(z)$. The stretching of the signal, substantial when CDP stacking is done over large offsets, was not compensated for by the migration procedure, which led to a distortion of the image of the upper boundary (fig. 3).

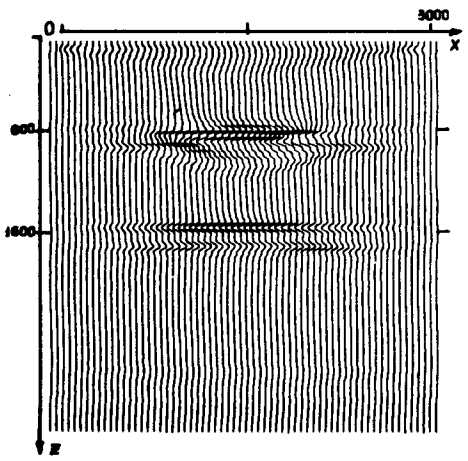

FIG. 3. The image obtained by the method "CDP stacking, wave migration"

Models 2-3. Closed smooth bodies in a homogeneous volume (planar case). Velocity in the outer medium: 3 km/sec, velocity within the objects: 2 km/sec in model 2 and 3.5 km/sec in model 3. Respective sizes of the bodies: 60×200 m and 100×150 m. Observation system: 64 receivers and 64 sources spaced 12.5 m apart, located on the line $z = 0$.

The computation of the wave field was carried out by the method of boundary integral equations, with the exception of the direct field due to sources at observation points [12]. The frequency range of 17 to 100 Hz was represented by 64 values. The image was formed on

a grid of 128×128 values with step sizes $\Delta x = \Delta z = 6.25$ m. The reconstruction was carried out in two stages: first the image was constructed using the known velocity in the outer medium -- 3 km/s. From this image the position of the upper boundary of the objects was determined, and there was carried out a recomputation of the wavefield on a horizontal line close to this boundary. After this, using the velocity for the interior of the object, the lower boundary was imaged. For a more precise reconstruction it is necessary to recompute the field directly on the chosen boundary of the section. Results of the reconstruction of the image are given in figs. 4 and 5, where the real positions of the objects are indicated by dashed lines. We should note that the absence of some of the elements of the boundaries on the image is caused by the fact that the rays reflected from these boundaries do not strike our observation system.

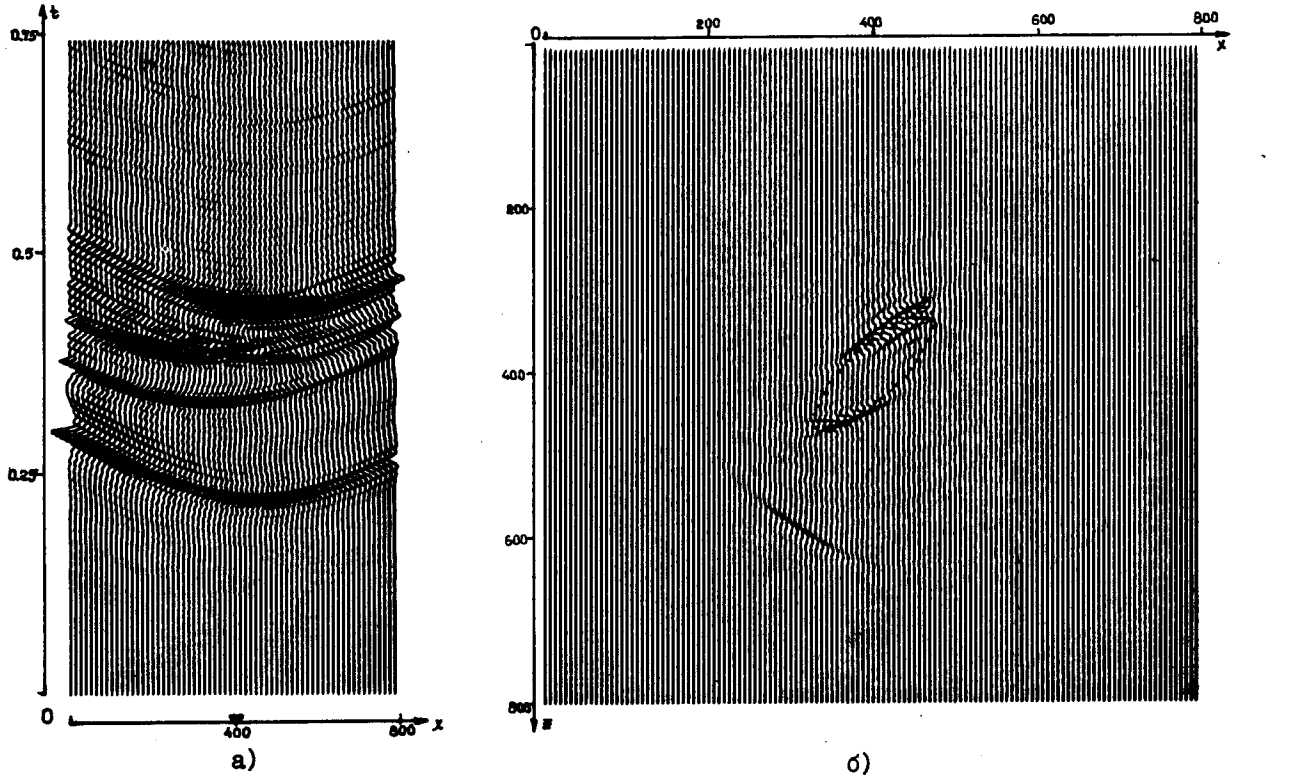

FIG. 4. (a) is a common-shot gather from model 2 (the source is at the 400 meter point). (b) is the result of imaging the object in model 2.

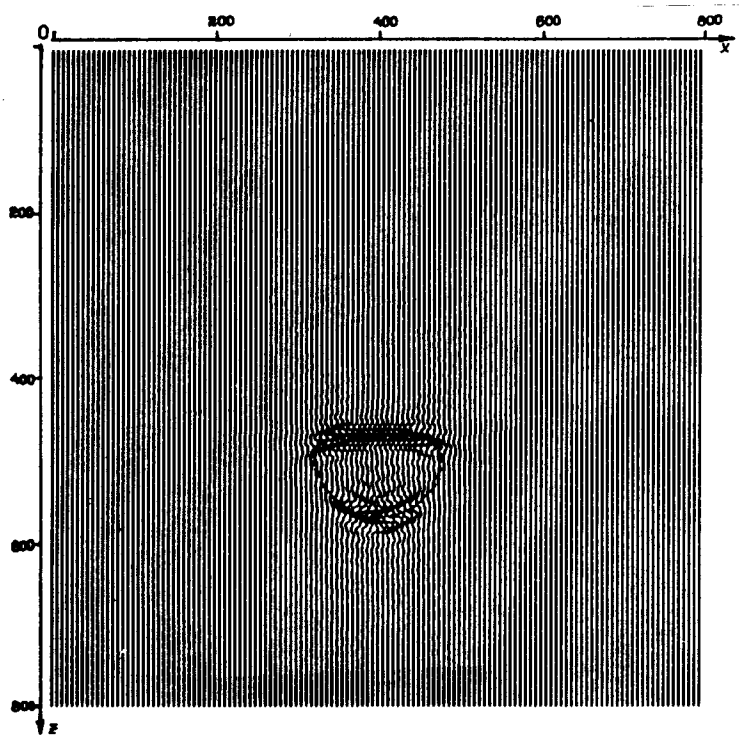

FIG. 5. Reconstructed image of model 3.

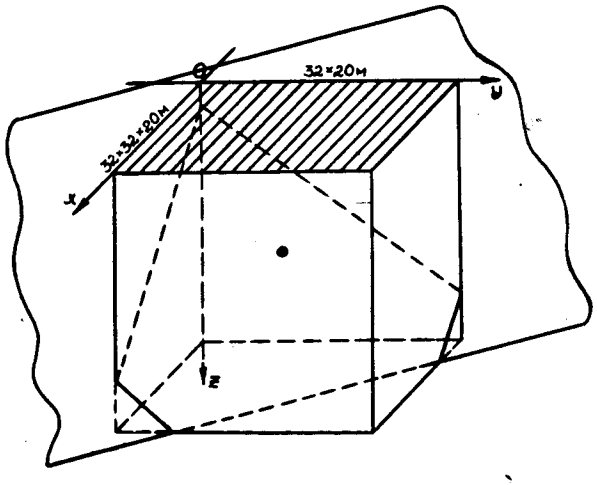

FIG. 6. Geometry of the three-dimensional model

Model 4. A specular reflecting plane with a dip of 45° to the vertical, and a small point scatterer above it. The observation system: on the plane $z = 0$ are 32 parallel profiles, heading at an angle of 45° to the strike line of the reflecting boundary. Each profile is composed of 32 sources and 32 receivers, with a step size $\Delta x = \Delta x_0 = 20$ m; the offset between profiles, $\Delta y = 20$ m.

The field reflected from the specular boundary was calculated by the method of virtual sources, while the scattering from the inhomogeneity was represented by the field from a point-like secondary radiator. The velocity in the medium was 2 km/sec, and the spectrum of the field was represented by 75 values in the range of 1 to 48 Hz. The geometry of the model is shown in fig. 6.

The image was formed on a three-dimensional 64×64×64 grid, with step sizes $\Delta x = \Delta y = \Delta z = 10$ m. From the resulting data we selected and imaged sections along various planes. In figs. 7-9 are presented the results of imaging along the 3 planes $x, y, z = 300$ m, all of which pass through the scattering inclusion. The geometry of all the images agrees with the original model. Because of the cyclicity of the convolution, which was carried out by means of the discrete Fourier transform, we can see the effect of the cyclicity of the image on those parts of the reflecting plane that extend beyond the limits of the observation system. This effect is easily removed by padding the original matrix with a field of zeroes, but doing this leads to an increase in the time of convolution which is significant in the three-dimensional case.

For a comparison to the full system of observation we chose a profile that lay over the point scatterer, and the data from this profile was processed using the two-dimensional variant of the algorithm. The result of this processing is shown in fig. 10. The image of the reflecting plane appears to be displaced and rotated relative to its actual position, which is indicate by the dotted line. Besides this, the image of the scatterer is distorted, and its relative intensity is noticeably lower, in comparison with the three-dimensional analog of the image. We should also note a numerical experiment that was carried out with the goal of examining the effect of the stationary phase approximations. We compared the results of processing data from an areal model using the corresponding algorithms, with the results from using its two-dimensional point source analog. The comparison showed that the distortion apparent in the second case was insignificant and had a low-frequency character, that is, it was determined by that part of the temporal spectrum of the field for which using the stationary phase method is incorrect.

Although the numerical experiments were carried out using data from observation systems that had fixed recording stations for all the shot locations, the algorithms can, without fundamental changes, be applied to the case usually found in practice for systems of multi-

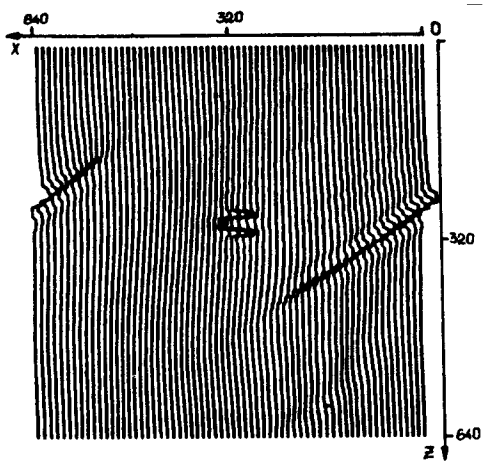

FIG. 7. Vertical section along the plane y = 300 m.

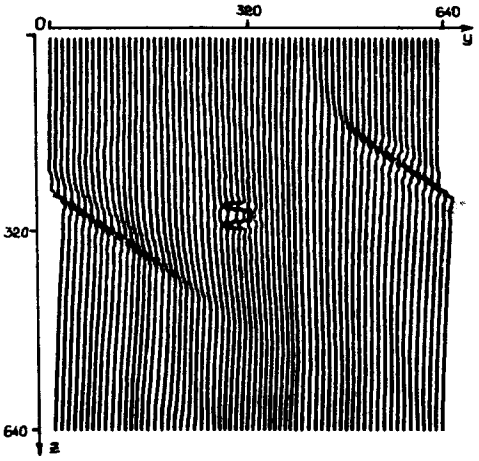

FIG. 8. Vertical section along the plane x = 300 m.

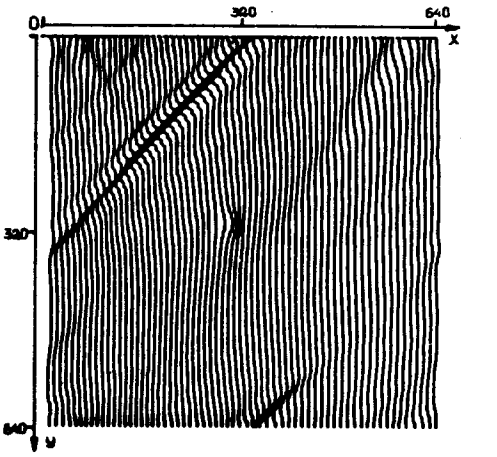

FIG. 9. Horizontal section along the plane z = 300 m.

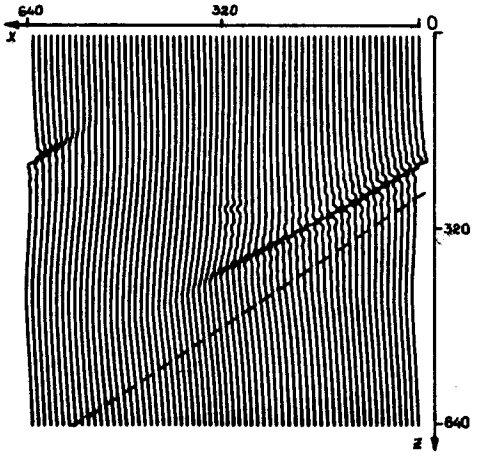

FIG. 10. The image obtained using a single profile

fold coverage.

In conclusion I would like to thank my co-workers at the Computing Center of the Siberian Branch of the USSR Academy of Science, V.N. Martynov and V.V. Voronin, who used the actual programs for the computation of the solution of the forward dynamic wave propagation problem in inhomogeneous media, and corresponding-member of the Academy A.S. Alekseev, to whom I am indebted for his constant attention and participation, which in many ways led to the realization of this work.

REFERENCES

Литература

I. Алексеев А.С., Цибульчик Г.М. О связи обратных задач теории распространения волн с задачами визуализации волновых полей.- Докл. АН СССР, I978, т.242, № 5, с. I030–I033.
2. Алексеев А.С., Жерняк Г.Ф. Многочастотный метод визуализации объектов и его опробование на полевом материале. -Геология и геофизика, I980, № 4, с. 58–67.
3. Бреховских Л.М. Волны в слоистых средах. - М.: Наука, I973. - 343 с.
4. Владимиров В.С. Уравнения математической физики. - М.: Наука, I967. - 528 с.
5. Запреев А.С., Чеверда В.А. О некоторых обратных задачах для волнового уравнения. - В кн.: Математические методы решения прямых и обратных задач геофизики. Новосибирск, ВЦ СО АН СССР, I98I, с.39-54.
6. Бейтман Г., Эрдейн А. Высшие трансцедентные функции. - М.: Наука, I974, т.2. - II3 с.
7. Бейтман Г., Эрдейн А. Таблицы интегральных преобразований- М.: Наука, I969, с. 58–6I.
8. Cohen J., Bleistein N. Velocity intervision procedure for acoustic waves. - Geophysics, 1979, v. 44, N 6, pp. 1077-1087.
9. Raz S. Three-dimensional velocity profile inversion from finitoffset scattering data. - Geophysics, 1981, v. 46, N 6, pp. 837-842.
I0. Clayton R., Stolt R. S Born-WKBJ inversion method for acoustic reflection data. - Geophysics, 1981, v. 46, N 11, pp. 1559-1567.
II. Алексеев А.С., Михайленко Б.Г. Метод вычисления теоретических сейсмограмм для сложно-построенных моделей сред.- Докл. АН СССР, I977, т.235, с. 46–49.
I2. Воронин В.В. Численное решение двумерной задачи дифракции упругой волны на упругом теле. Препринт № I23. - Новосибирск, I978. - 26 с. - В надзаг. ВЦ СО АН СССР.

The first earth colony on Mars has been swept away by an epidemic of Barsoomian flu. The cause: a native Martian virus not yet isolated.

There is no way to identify a newly infected person until the symptoms appear weeks later. The flu is highly contagious, but only by direct contact. The virus transfers readily from flesh to flesh, or from flesh to any object which in turn can contaminate any flesh it touches.

Ms. Hooker, director of the colony, has been seriously injured in a rocket accident. Three immediate operations are required. The first will be per- formed by Dr. Xenophone, the second by Dr. Ypsilanti, the third by Dr. Zeno. Any of the surgeons may be infected with Barsoomian flu. Ms. Hooker, too, may have caught the disease.

Just before the first operation, it is discovered that the colony's hospital has only two pairs of sterile surgeon's gloves. No others are obtainable, and there is no time for resterilizing. Each surgeon must operate with both hands.

"I don't see how we can avoid the risk of one of us becoming infected," said Dr. Xenophon to Dr. Zeno. "When I operate, my hands may contaminate the insides of my gloves. Ms. Hooker's body may contaminate the outsides. The same thing will happen to gloves worn by Dr. Ypsilanti. When it's your turn, you'll have to wear gloves that could be contaminated on both sides."

"Not so," says Dr. Zeno, who had taken a course in topology when he was a young medical student in Paris. "There's a simple procedure that will eliminate all risk of any of us catching the flu from one another or from Ms. Hooker."

What does Dr. Zeno have in mind?

##########

An iron bar, 13 inches long, is marked in four places: 1, 2, 6, and 10 inches from one of the ends. Of what special use is the bar?

##########

What is the lowest number whose English name contains the letter 'a'?

##########

Dick's age is twice what Tom's was when Dick's was twice what Tom's was when Dick's was three years more than Tom's was when Dick's was both thrice what it was when Tom was born and three quarters of Tom's present age. What will Tom's be when Dick's is twice what Tom's will be when Dick's is the sum of both their present ages?

##########